

# The Proton Electric Pygmy Dipole Resonance

N. Paar

*Institut für Kernphysik, Technische Universität Darmstadt,*

*Schlossgartenstrasse 9, D-64289 Darmstadt, Germany*

D. Vretenar

*Physics Department, Faculty of Science, University of Zagreb, Croatia*

P. Ring

*Physik-Department der Technischen Universität München, D-85748 Garching, Germany*

(Dated: May 10, 2019)

## Abstract

The evolution of the low-lying E1 strength in proton-rich nuclei is analyzed in the framework of the self-consistent relativistic Hartree-Bogoliubov (RHB) model and the relativistic quasiparticle random-phase approximation (RQRPA). Model calculations are performed for a series of  $N=20$  isotones and  $Z=18$  isotopes. For nuclei close to the proton drip-line, the occurrence of pronounced dipole peaks is predicted in the low-energy region below 10 MeV excitation energy. From the analysis of the proton and neutron transition densities and the structure of the RQRPA amplitudes, it is shown that these states correspond to the proton pygmy dipole resonance.

PACS numbers: 21.10.Gv, 21.30.Fe, 21.60.Jz, 24.30.Cz

A number of experimental and theoretical studies of the multipole response of exotic nuclei far from stability have been reported in recent years. On the neutron-rich side, in particular, the possible occurrence of the pygmy dipole resonance (PDR), i.e. the resonant oscillation of the weakly-bound neutron skin against the isospin saturated proton-neutron core, has been investigated. The onset of low-lying E1 strength has been observed not only in exotic nuclei with a large neutron excess, e.g. for neutron-rich oxygen isotopes [1], but also in stable nuclei with moderate proton-neutron asymmetry, like  $^{44,48}\text{Ca}$  and  $^{208}\text{Pb}$  [2, 3, 4]. On the theory side, various models have been employed in the investigation of the nature of the low-lying dipole strength. Recent studies include the application of the Skyrme Hartree-Fock + quasiparticle RPA with phonon coupling [5, 6], the time-dependent density-matrix theory [7], the continuum linear response in the coordinate-space Hartree-Fock Bogoliubov formalism [8], the quasiparticle phonon model [2, 3, 9, 10], the relativistic RPA [11, 12], and the relativistic quasiparticle RPA (RQRPA) [13, 14]. The PDR is interesting not only as a new and exotic mode of nuclear excitations, but it also plays an important role in predictions of neutron capture rates in the r-process nucleosynthesis, and consequently in the calculated elemental abundance distribution. Even though the E1 strength of the PDR is small compared to the total dipole strength, the occurrence of the PDR significantly enhances the radiative neutron capture cross section on neutron-rich nuclei, as shown in recent large-scale QRPA calculations of the E1 strength for the whole nuclear chart [15, 16].

In the analysis based on the relativistic (Q)RPA [11, 12, 13, 14], it has been shown that in neutron-rich nuclei the electric dipole response is characterized by the fragmentation of the strength distribution and its spreading into the low-energy region. In light nuclei, the low-lying dipole strength is not collective and originates from non-resonant single-neutron excitations. In medium-heavy and heavy neutron-rich nuclei, on the other hand, some of the low-lying dipole states display a more distributed structure of the RQRPA amplitudes. The study of the corresponding transition densities and velocity distributions revealed the dynamics of the neutron pygmy dipole resonance.

In this work we employ the relativistic QRPA in the study of the evolution of low-lying dipole strength in proton-rich nuclei. Because the proton drip-line is much closer to the line of  $\beta$ -stability than the neutron drip-line, bound nuclei with an excess of protons over neutrons can be only found in the region of light  $Z \leq 20$  and medium mass  $20 < Z \leq 50$  elements. For  $Z > 50$ , nuclei in the region of the proton drip-line are neutron-deficient rather

than proton-rich. In addition, in contrast to the evolution of the neutron skin in neutron-rich systems, because of the presence of the Coulomb barrier nuclei close to the proton drip-line generally do not exhibit a pronounced proton skin, except for very light elements. Since in light nuclei the multipole response is generally less collective, all these effects seem to preclude the formation of the pygmy dipole states in nuclei close to the proton drip-line. Nevertheless, the present analysis will show that proton pygmy dipole states can develop in light and medium mass proton-rich nuclei.

The relativistic QRPA [13] is formulated in the canonical single-nucleon basis of the relativistic Hartree-Bogoliubov (RHB) model and is fully self-consistent. For the interaction in the particle-hole channel effective Lagrangians with nonlinear meson self-interactions or density-dependent meson-nucleon couplings are used, and pairing correlations are described by the pairing part of the finite-range Gogny interaction. Both in the particle-hole and pairing channels, the same interactions are used in the RHB equations that determine the canonical quasiparticle basis, and in the matrix equations of the RQRPA. This feature is essential for the decoupling of the zero-energy mode which corresponds to the spurious center-of-mass motion. In addition to configurations built from two-quasiparticle states of positive energy, the RQRPA configuration space contains quasiparticle excitations formed from the ground-state configurations of fully or partially occupied states of positive energy and the empty negative-energy states from the Dirac sea. In the present analysis of the dipole response of proton-rich nuclei in the fully self-consistent RHB+RQRPA framework, the density-dependent effective interaction DD-ME1 [17] is employed in the *ph*-channel, and the finite range Gogny interaction D1S [18] in the *pp*-channel.

In Fig. 1 we display the RQRPA dipole strength distributions in the  $N=20$  isotones:  $^{40}\text{Ca}$ ,  $^{42}\text{Ti}$ ,  $^{44}\text{Cr}$ , and  $^{46}\text{Fe}$ . The electric dipole response

$$B^T(EJ, \omega_\nu) = \frac{1}{2J_i+1} \left| \sum_{\mu\mu'} \left\{ X_{\mu\mu'}^{v,J0} \langle \mu || \hat{Q}_J^T || \mu' \rangle + (-1)^{j_\mu - j_{\mu'} + J} Y_{\mu\mu'}^{v,J0} \langle \mu' || \hat{Q}_J^T || \mu \rangle \right\} (u_\mu v_{\mu'} + (-1)^J v_\mu u_{\mu'}) \right|^2 , \quad (1)$$

is calculated for the isovector dipole operator

$$\hat{Q}_{1\mu}^{T=1} = \frac{N}{N+Z} \sum_{p=1}^Z r_p Y_{1\mu} - \frac{Z}{N+Z} \sum_{n=1}^N r_n Y_{1\mu} . \quad (2)$$

For each RQRPA energy  $\omega_\nu$ ,  $X^\nu$  and  $Y^\nu$  denote the corresponding forward- and backward-going two-quasiparticle amplitudes, respectively.  $v_\mu$  and  $u_\mu$  are the occupation numbers of

the single-particle levels in the canonical basis. The discrete spectra are averaged with the Lorentzian distribution

$$R(E) = \sum_i B(E1, 1_i \rightarrow 0_f) \frac{\Gamma/2\pi}{(E - E_i)^2 + \Gamma^2/4}, \quad (3)$$

with  $\Gamma = 1$  MeV as an arbitrary choice for the width of the Lorentzian.

The dipole strength distributions in Fig. 1 are dominated by the isovector giant dipole resonances (GDR) at  $\approx 20$  MeV excitation energy. In these relatively light systems the GDR still exhibits pronounced fragmentation. With the increase of the number of protons, low-lying dipole strength appears in the region below the GDR and, for  $^{44}\text{Cr}$  and  $^{46}\text{Fe}$ , a pronounced low-energy peak is found at  $\approx 10$  MeV excitation energy. What is the nature of this low-lying dipole state? In the lower panel of Fig. 1 we plot the proton and neutron transition densities for the peaks at 10.15 MeV in  $^{44}\text{Cr}$  and 9.44 MeV in  $^{46}\text{Fe}$ , and compare them with the transition densities of the GDR state at 18.78 MeV in  $^{46}\text{Fe}$ . Obviously the dynamics of the two low-energy peaks is very different from that of the isovector GDR: the proton and neutron transition densities are in phase in the nuclear interior and there is almost no contribution from the neutrons in the surface region. The low-lying state does not belong to statistical E1 excitations sitting on the tail of the GDR, but represents a fundamental mode of excitation: the proton electric pygmy dipole resonance (PDR).

In Fig. 2 we analyze the RQRPA structure of the dipole response in  $^{46}\text{Fe}$ . This nucleus is located at the proton drip-line (see Ref. [19] for a recent review on the limits of nuclear stability) and, very recently, for the first time evidence for ground-state two-proton radioactivity was reported in the decay of  $^{45}\text{Fe}$  [20, 21]. The discrete unperturbed Hartree-Bogoliubov and full RQRPA E1 spectra of  $^{46}\text{Fe}$  are shown in the left panel. Since the interaction is repulsive in the isovector channel, one expects that the inclusion of the residual interaction will result in the shift of the full RQRPA spectrum to higher energies with respect to the unperturbed spectrum. This is clearly the case for the states in the GDR region. The lowest group of states at  $\approx 10$  MeV, however, gains strength and is shifted to lower energy. Obviously the nature of these states is not isovector. The QRPA structure of these states is shown in the panel on the right, where for the three low-lying states at 9.02, 9.44, and 10.26 MeV, as well as for the strongest state in the GDR region at 18.78 MeV, we plot the corresponding QRPA amplitude of proton and neutron  $2qp$  configurations

$$\xi_{2qp} = \left| X_{2qp}^\nu \right|^2 - \left| Y_{2qp}^\nu \right|^2, \quad (4)$$

with the normalization condition

$$\sum_{2qp} \xi_{2qp} = 1. \quad (5)$$

For each of the four dipole states, in addition to the excitation energy we have also included the corresponding  $B(E1)$  value. The QRPA amplitudes are shown in a logarithmic plot as functions of the unperturbed energy of the respective  $2qp$ -configurations. Only amplitudes which contribute more than 0.01% are shown, and we also differentiate between proton and neutron configurations. We note that, rather than a single proton  $2qp$  excitation, the low-lying states are characterized by a superposition of a number of  $2qp$  configurations. Obviously the pygmy states display a degree of collectivity that can be directly compared with the QRPA structure of the GDR state at 18.78 MeV. In addition, proton  $2qp$  configurations account for  $\approx 99\%$  of the QRPA amplitude of the pygmy states, whereas the ratio of the proton to neutron contribution to the GDR state is  $\approx 2$ . For the GDR states the  $2qp$  configurations predominantly correspond to excitations from the  $sd$ -shell to the  $fp$ -shell. The structure of the pygmy states, on the other hand, is dominated by transitions from the  $1f_{7/2}$  proton state at -0.17 MeV, and from the  $2p_{3/2}$  proton state at 3.60 MeV (this state is only bound because of the Coulomb barrier). The energy weighted sum of the strength below 11 MeV excitation energy corresponds to 2.5% of the Thomas-Reiche-Kuhn sum rule (TRK).

Another example of particularly pronounced proton PDR are the proton-rich isotopes of Ar. In the left panel of Fig. 3 we display the RHB+RQRPA electric dipole strength distribution in  $^{32}\text{Ar}$ . In addition to the rather fragmented GDR structure at  $\approx 20$  MeV, prominent proton PDR peaks are obtained just below 10 MeV. For the four states at 8.30, 8.94, 9.36, and 9.60 MeV, which constitute the pygmy structure, in Fig. 4 we plot the proton and neutron transition densities, and the distributions of the RQRPA amplitudes, in comparison with the GDR state at 18.01 MeV. In contrast to the isovector GDR, the proton and neutron transition densities of the pygmy states are in phase. The RQRPA amplitudes of the low-lying states present superpositions of many proton  $2qp$  configurations, with the neutron contributions at the level of 1%. The dominant configurations correspond to transitions from the proton states  $1d_{3/2}$  at -2.09 MeV and  $2s_{1/2}$  at -4.07 MeV. The corresponding  $B(E1)$  values are included in Fig. 4. The energy weighted sum of the strength below 10 MeV takes 5.6% of the TRK sum rule. In the right panel of Fig. 3 we display the mass dependence of the centroid energy of the pygmy peaks and the corresponding values

of the integrated  $B(E1)$  strength below 10 MeV excitation energy. In contrast to the case of medium-heavy and heavy neutron-rich isotopes, in which both the PDR and GDR are lowered in energy with the increase of the neutron number [14], in proton-rich isotopes the mass dependence of the PDR excitation energy and  $B(E1)$  strength is opposite to that of the GDR. The proton PDR decreases in energy with the growth of the proton excess. This mass dependence is intuitively expected since, as we have shown, the proton PDR mode is dominated by transitions from the weakly-bound proton orbitals. As the proton drip-line is approached, either by increasing the number of protons or by decreasing the number of neutrons, due to the weaker binding of higher proton orbitals one expects more inert oscillations, i.e. lower excitation energies. The number of  $2qp$  configurations which include weakly-bound proton orbitals increases towards the drip-line, resulting in an enhancement of the low-lying  $B(E1)$  strength.

In conclusion, we have employed the self-consistent RHB model and the RQRPA in the analysis of the low-energy dipole response in proton-rich nuclei close to the proton drip-line. For nuclei with more protons than neutrons, in the chain of  $N=20$  isotones the RHB+RQRPA calculation predicts the occurrence of an exotic mode in the low-energy region below 10 MeV: the proton electric pygmy dipole resonance. The analysis of the corresponding proton and neutron transition densities shows that proton PDR states correspond to the oscillation of the proton excess against an approximately isospin-saturated core. The RQRPA amplitudes of the pygmy states display a superposition of many proton  $2qp$  configurations, whereas the contribution of neutron excitations is at the level of 1%. The dominant configurations include weakly-bound proton orbitals, and also the states which are bound only because of the presence of the Coulomb barrier. In contrast to the rather fragmented GDR, the PDR strength is concentrated in a narrow region of excitation energies well below the region of giant resonances, and the energy weighted sum of the PDR strength corresponds to a few percent of the TRK sum rule. With the decrease of the number of neutrons, for the chain of proton-rich Ar isotopes the proton PDR is lowered in energy, and the integrated  $B(E1)$  strength in the low-energy region increases accordingly. For heavier nuclei the proton drip-line is located in the region of neutron-deficient, rather than proton-rich nuclei, and therefore no low-lying dipole strength is calculated in medium-heavy and heavy nuclei close to the proton drip-line.

## ACKNOWLEDGMENTS

This work has been supported in part by the Bundesministerium für Bildung und Forschung - project 06 MT 193, by the Deutsche Forschungsgemeinschaft (DFG) under contract SFB 634, by the Croatian Ministry of Science - project 0119250, and by the Gesellschaft für Schwerionenforschung (GSI) Darmstadt.

---

- [1] A. Leistenschneider et al., Phys. Rev. Lett. 86, 5442 (2001).
- [2] N. Ryezayeva et al., Phys. Rev. Lett. 89, 272502 (2002).
- [3] J. Enders et al., Nucl. Phys. A 724, 243 (2003).
- [4] T. Hartmann et al., Phys. Rev. Lett. 93, 192501 (2004).
- [5] G. Coló and P. F. Bortignon, Nucl. Phys. A 696, 427 (2001).
- [6] D. Sarchi, P. F. Bortignon, and G. Coló, Phys. Lett. B 601, 27 (2004).
- [7] M. Tohyama and A. S. Umar, Phys. Lett. B 516, 415 (2001).
- [8] M. Matsuo, Nucl. Phys. A 696, 371 (2001).
- [9] N. Tsoneva, H. Lenske, and Ch. Stoyanov, Nucl. Phys. A 731, 273 (2004).
- [10] N. Tsoneva, H. Lenske, and Ch. Stoyanov, Phys. Lett. B 586, 213 (2004).
- [11] D. Vretenar, N. Paar, P. Ring, and G. A. Lalazissis, Phys. Rev. C 63, 047301 (2001).
- [12] D. Vretenar, N. Paar, P. Ring, and G. A. Lalazissis, Nucl. Phys. A 692, 496 (2001).
- [13] N. Paar, P. Ring, T. Nikšić, and D. Vretenar, Phys. Rev. C 67, 034312 (2003).
- [14] N. Paar, T. Nikšić, D. Vretenar, and P. Ring, Phys. Lett. B 606, 288 (2005).
- [15] S. Goriely and E. Khan, Nucl. Phys. A 706, 217 (2002).
- [16] S. Goriely, E. Khan, and M. Samyn, Nucl. Phys. A 739, 331 (2004).
- [17] T. Nikšić, D. Vretenar, P. Finelli, and P. Ring, Phys. Rev. C 66, 024306 (2002).
- [18] J. F. Berger, M. Girod, and D. Gogny, Comp. Phys. Comm. 63, 365 (1991).
- [19] M. Thoennessen, Rep. Prog. Phys. 67, 1187 (2004).
- [20] J. Giovinazzo et al., Phys. Rev. Lett. 89, 102501 (2002).
- [21] M. Pfutzner et al., Eur. Phys. J. A 14, 279 (2002).

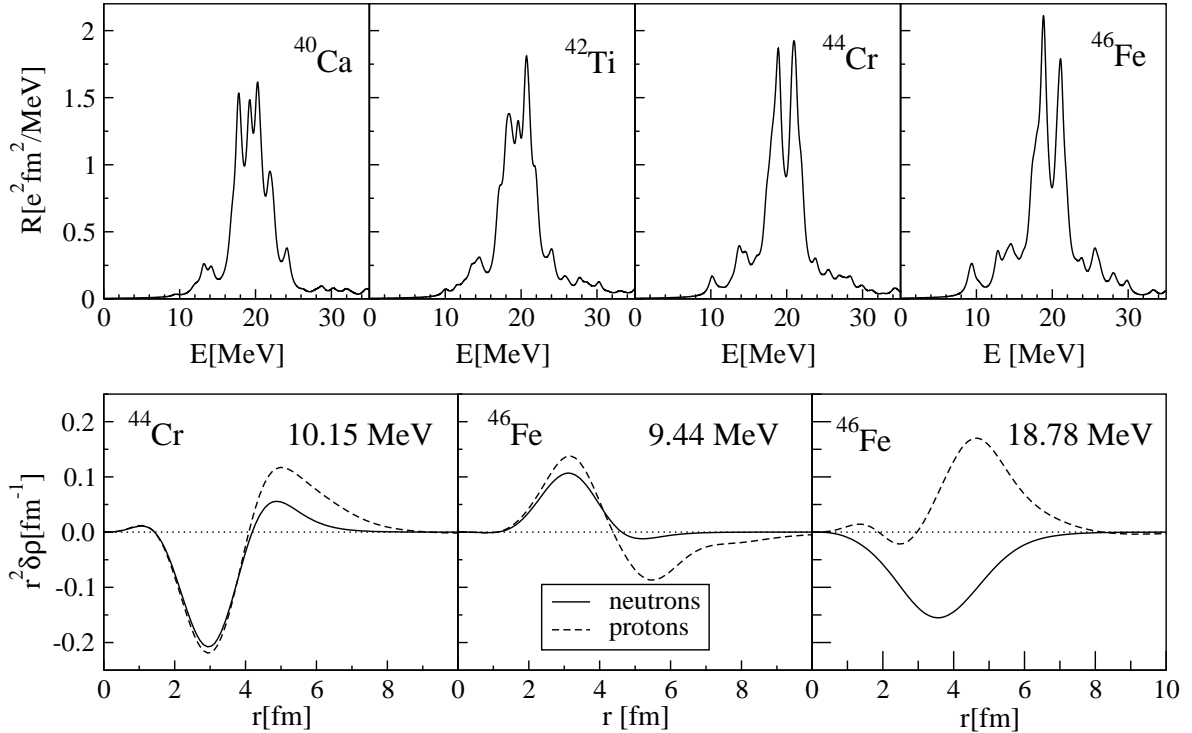


FIG. 1: The RHB+RQRPA isovector dipole strength distributions in the  $N=20$  isotones, calculated with the DD-ME1 effective interaction. For  $^{44}\text{Cr}$  and  $^{46}\text{Fe}$  the proton and neutron transition densities for the main peak in the low-energy region are displayed in the lower panel and, for  $^{46}\text{Fe}$ , the transition densities for the main GDR peak.

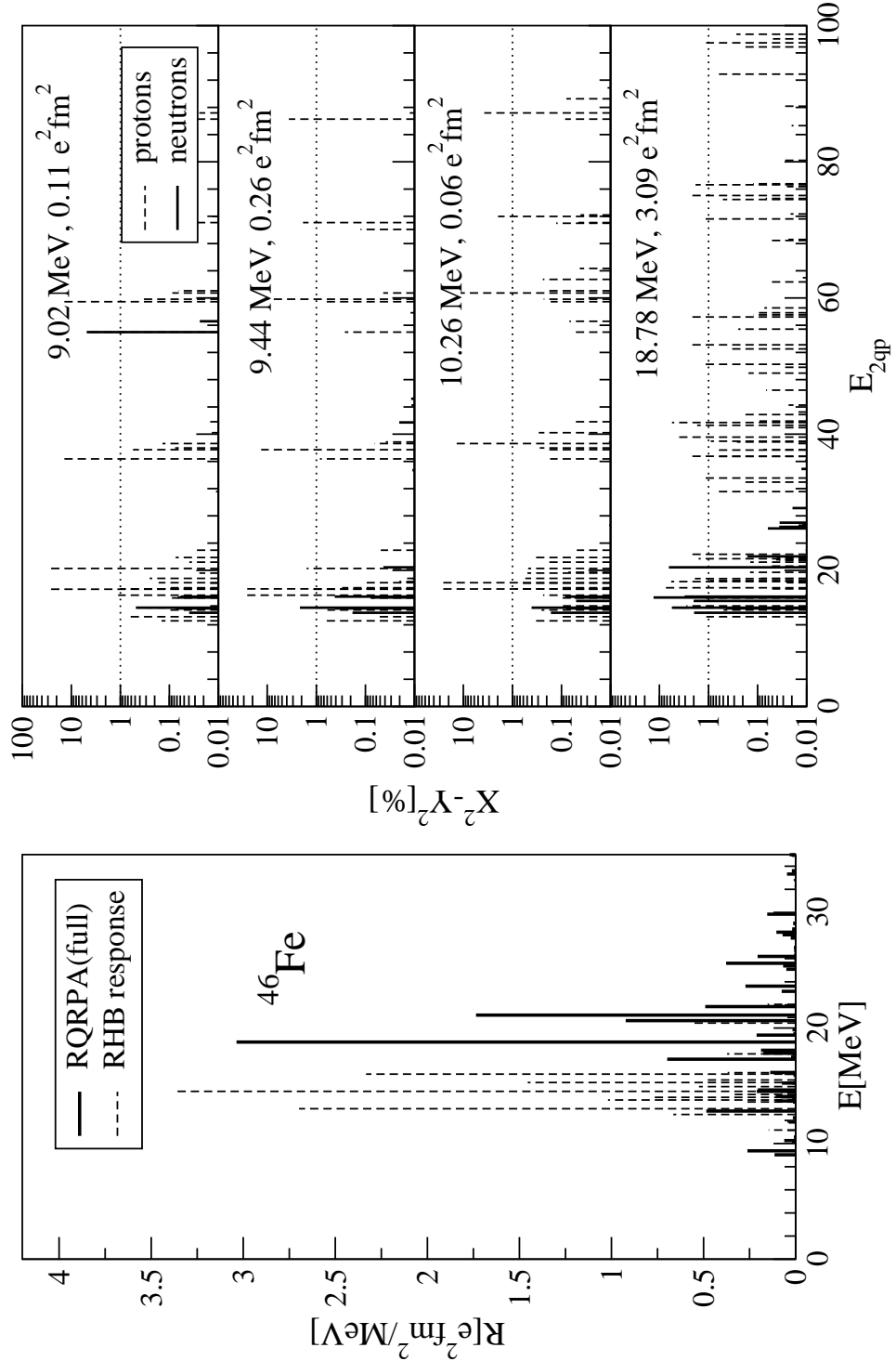


FIG. 2: The discrete Hartree-Bogoliubov and full RQRPA E1 spectra in  $^{46}\text{Fe}$  (left panel). For the main peaks in the low-energy region and in the region of the isovector GDR, the distributions of the RQRPA amplitudes are shown as functions of the unperturbed energy of the respective

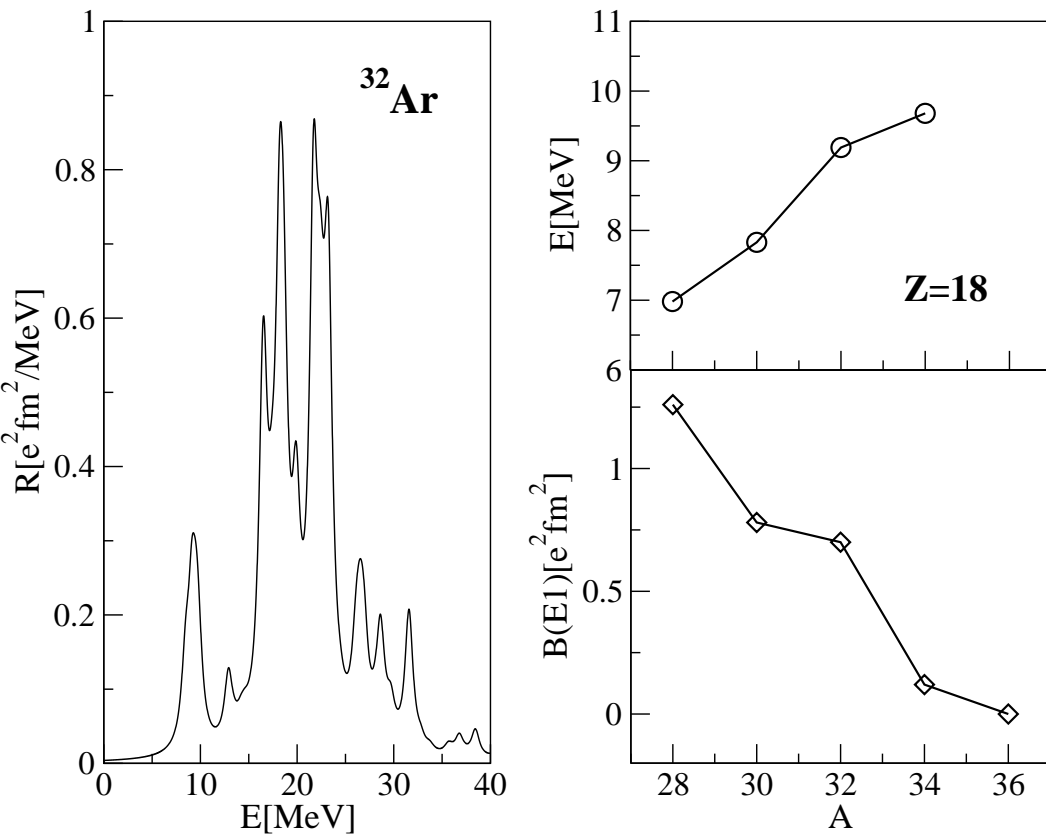


FIG. 3: The RHB+RQRPA isovector dipole strength distribution in  $^{32}\text{Ar}$  (left panel). For the argon isotopes, the mass dependence of the centroid energy of the pygmy peak and the corresponding values of the integrated  $B(E1)$  strength below 10 MeV excitation energy are shown in the panel on the right.

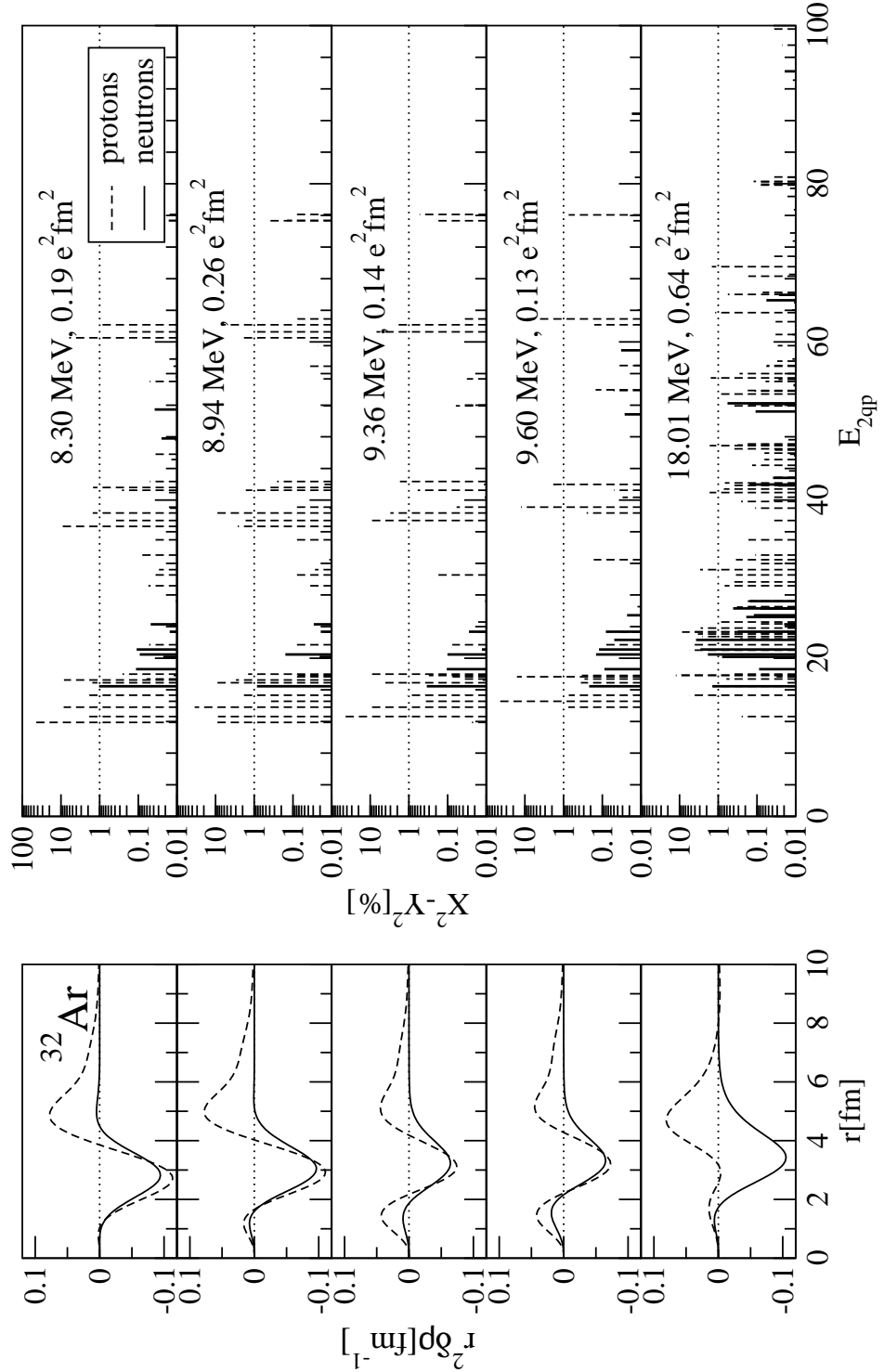


FIG. 4: Transition densities and RQRPA amplitudes for selected  $1^-$  states in  $^{32}\text{Ar}$ . For the main peaks in the low-energy region and in the region of the isovector GDR, the proton and neutron transition densities are shown in the left panel. The corresponding distributions of the RQRPA